

Communication

# Bond Memory in Dynamically-Determined Stereoselectivity

Vladislav A. Roytman, Shengfei Jin, Vu T. Nguyen, Viet D. Nguyen,  
Graham C. Haug, Oleg V. Larionov, and Daniel A. Singleton

*J. Am. Chem. Soc.*, **Just Accepted Manuscript** • DOI: 10.1021/jacs.9b12227 • Publication Date (Web): 19 Dec 2019

Downloaded from [pubs.acs.org](https://pubs.acs.org) on December 19, 2019

## Just Accepted

"Just Accepted" manuscripts have been peer-reviewed and accepted for publication. They are posted online prior to technical editing, formatting for publication and author proofing. The American Chemical Society provides "Just Accepted" as a service to the research community to expedite the dissemination of scientific material as soon as possible after acceptance. "Just Accepted" manuscripts appear in full in PDF format accompanied by an HTML abstract. "Just Accepted" manuscripts have been fully peer reviewed, but should not be considered the official version of record. They are citable by the Digital Object Identifier (DOI®). "Just Accepted" is an optional service offered to authors. Therefore, the "Just Accepted" Web site may not include all articles that will be published in the journal. After a manuscript is technically edited and formatted, it will be removed from the "Just Accepted" Web site and published as an ASAP article. Note that technical editing may introduce minor changes to the manuscript text and/or graphics which could affect content, and all legal disclaimers and ethical guidelines that apply to the journal pertain. ACS cannot be held responsible for errors or consequences arising from the use of information contained in these "Just Accepted" manuscripts.

# Bond Memory in Dynamically-Determined Stereoselectivity

Vladislav A. Roytman,<sup>†</sup> Shengfei Jin,<sup>†</sup> Vu T. Nguyen,<sup>†</sup> Viet D. Nguyen,<sup>†</sup> Graham C. Haug,<sup>†</sup> Oleg V. Larionov,<sup>\*,†</sup> and Daniel A. Singleton<sup>\*,†</sup>

<sup>†</sup>Department of Chemistry, Texas A&M University, P.O. Box 30012, College Station, Texas 77842, United States

<sup>\*</sup>Department of Chemistry, The University of Texas at San Antonio, San Antonio, Texas 78249, United States

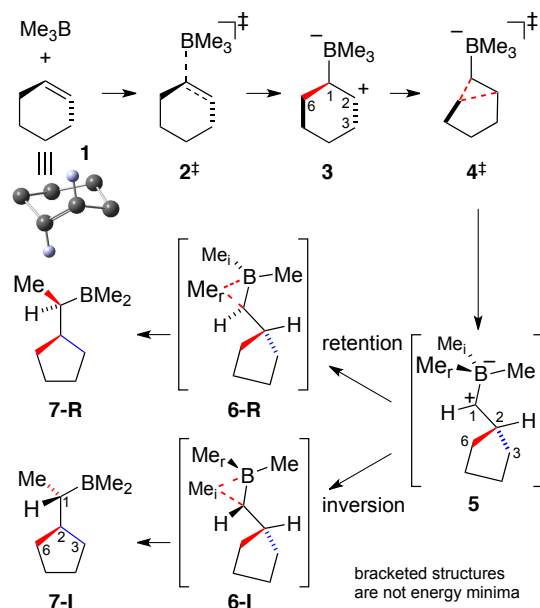
Supporting Information Placeholder

**ABSTRACT:** The carboborative ring contraction of cyclohexenes exhibits an abnormal selectivity pattern in which a formally concerted double-migration gives rise to predominant but not exclusive inversion products. In dynamic trajectories, the inversion and retention products are formed from the same transition state, and the trajectories accurately account for the experimental product ratios. The unusual origin of the selectivity is the dynamically retained non-equivalence of newly-formed versus preexisting bonds after the first bond migration.

Much of the understanding of molecular structure in chemistry implicitly assumes time-averaged geometries and statistical distributions of energy in molecules. For example, symmetry-linked bonds to atoms are considered equivalent, even though in individual molecules at any instant the positions and energies of the atoms may be inequivalent.  $\text{CH}_2\text{FCl}$  is not viewed as being chiral in any meaningful sense, because no ordinary experiment can detect the ephemeral positional and energetic differences between the hydrogen atoms.<sup>1</sup> On sufficiently short time scales, however, the *de facto* dynamical asymmetry of structures with symmetrical connectivity can influence experimental observations, either through bond breaking in specifically energized fragments of molecules<sup>2,3</sup> or through dynamic matching.<sup>4,5,6,7,8,9</sup> We describe here how the combination of energetic non-equivalence in newly-formed versus preexisting bonds and the initial geometrical non-equivalence of the two bonds on the slope of an energy surface can direct high stereoselectivity at an adjacent reactive center.

The Larionov group recently reported the photoinduced carboborative ring contraction of cyclohexenes to afford chiral cyclopentanes.<sup>10</sup> The reaction was proposed to occur by a sensitized *cis* / *trans* isomerization, giving rise to a strained *trans*-cyclohexene nucleophile (**1**). Electrophilic addition by a tertiary borane via **2**<sup>‡</sup> then forms the zwitterionic adduct **3**. Ring-contraction through **4**<sup>‡</sup> leads to the betaine structure **5**. The nature of **5** and its dynamics will be of central importance here. Stereodivergent alkyl migrations via **6-R** or **6-I** quench the charge separation and give the product cyclopentanes **7-R** and **7-I**. The stereochemistry of the combination of ring-contraction and boron-alkyl migration steps can-

not be determined with cyclohexene itself, but a strong preference for inversion was previously seen with complex substrates. Here, we have carefully assigned and quantitated the relatively simple (+)-limonene reaction (Figure 1).



An unusual observation is that the two rearrangement steps are stereochemically linked, but not completely so. That is, if the bond to  $\text{C}_6$  lost in the ring-contraction step is viewed as the “leaving group” and the migrating boron-alkyl is the “nucleophile”, the combination of steps converting **3** to **7** occurs with preferential, but not exclusive, inversion of configuration at  $\text{C}_1$  (see **9-I** / **10-I** versus **9-R** / **10-R** in Figure 1). If the two migrations occurred simultaneously, stereospecific inversion would be expected, as in any  $\text{S}_{\text{N}}2$  step. If the ring-contraction step were complete before the boron-alkyl migration, equal inversion and retention might be expected. The high stereoselectivity but absence of  $\text{S}_{\text{N}}2$ -like stereospecificity then appears inconsistent with either a concerted or a two-step process.

Our hypothesis was that this unexpected stereoselectivity pattern is associated with dynamics on a bifurcating energy surface.<sup>11,12,13,14</sup> The trajectory study here supports this idea, but uncovers an origin for the selectivity that is uniquely dynamical in nature. The results complicate the mechanistic interpretation of stereoselectivity in reactions.

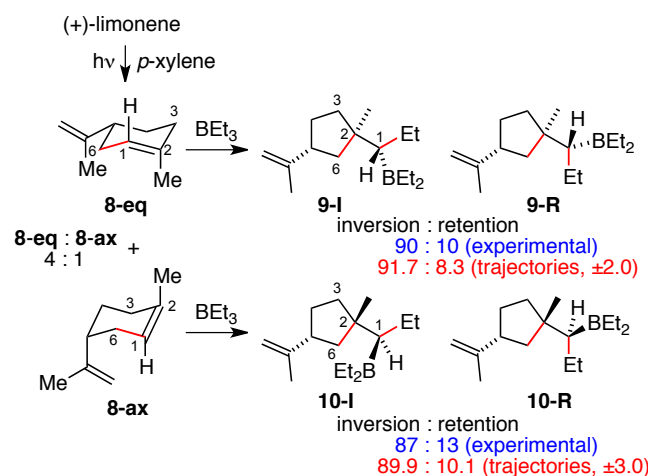


**Figure 1.** Stereochemistry of the photoinduced carboborative ring contraction of (+)-limonene. See the SI for the determination of the experimental ratios.

M11/6-31+G\*\* calculations were chosen here based on a comparison of diverse DFT methods versus DLPNO-CCSD(T)/aug-cc-pVTZ energies for a series of geometries along a minimum energy path (MEP) from **1** to **7** (see the Supporting Information (SI)). The ring contraction of **3** is barrierless,<sup>15</sup> and the MEP has C<sub>6</sub> migrate from C<sub>1</sub> to C<sub>2</sub> to pass into the area of structure **5**, though **5** is not an energy minimum. The MEP then continues downhill by a boron-alkyl shift to C<sub>1</sub> through **6-I** to afford **7-I**. The energy surface for the ring contraction and boron-alkyl migration is steeply declining, going downhill by 61 kcal/mol overall and 45 kcal/mol from **5** to **7-I**.

The stereochemically tractable (+)-limonene / triethylborane reaction of Figure 1 was the focus of the calculations here. Unlike the model reaction, this system is configurationally and conformationally complex. The initial *cis* / *trans* isomerization can occur in two ways, leading to a distorted chair with the isopropenyl group either equatorial (**8-eq**) or axial (**8-ax**). For each, the isopropenyl group and the attacking triethylborane can adopt multiple conformations, and the possibilities were explored systematically (see the SI). Importantly, the conformation of the triethylboryl group later in the mechanism is established in the transition state for its attack on the alkene. The structures subsequent to the initial addition step are extremely short-lived. As a result, their conformations are in a non-Curtin-Hammett regime<sup>16</sup> and they cannot interconvert prior to the final product formation.

Figure 2 outlines the calculated mechanism. The lowest-energy TS **11<sup>‡</sup>** for the addition of triethylborane to **8-eq** involves a low barrier (8.0 kcal/mol in free energy) despite the steric hindrance. The resulting zwitterion **12** exists in a shallow energy well of only 0.3 kcal/mol versus the subsequent ring-contraction TS **13<sup>‡</sup>**. The MEP forward from **13<sup>‡</sup>** faces no further barrier before arriving at the inversion product **9-I**, so in this respect the two rearrangement steps are concerted. However, the ring contraction is complete in the MEP before any significant motion of a boron-ethyl group, and the MEP passes through the shoulder structure **14** (the limo-

nene analog of **5**, not an energy minimum). Because of the tertiary cation at C<sub>2</sub> in **12**, the ring contraction is less favored than in the unsubstituted model, and it is only ~2.8 kcal/mol downhill from **12** to **14**. The final boron-alkyl migration is extremely exothermic. No TS leading by MEP to **9-R** could be located, and the same was true for the other conformations explored. This absence of TSs leading to retention means that conventional stationary-point calculations cannot account for the experimentally observed minor product.

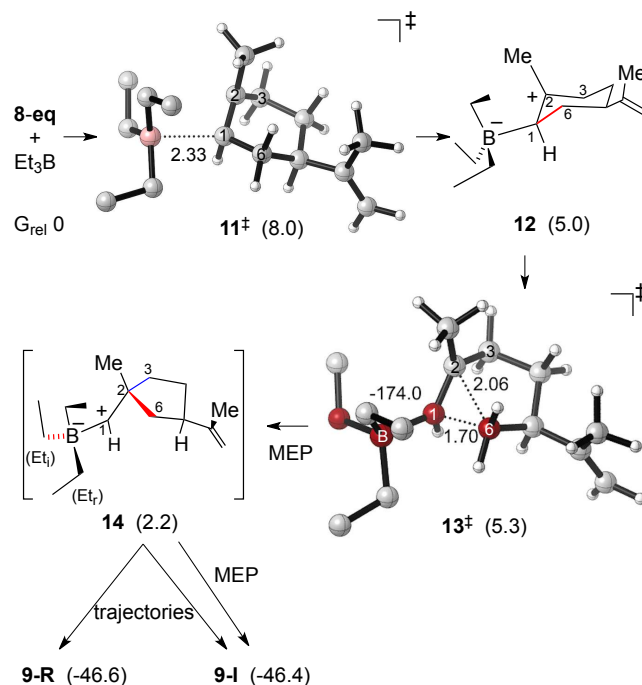


**Figure 2.** Lowest-energy calculated mechanism for the reaction of **8-eq** with triethylborane. Relative free energies are shown in parentheses in kcal/mol. The energy for non-minimum **14** is based on when the C<sub>2</sub>–C<sub>6</sub> distance is 1.6 Å.

To explore whether the retention product could arise from dynamic motions after the ring contraction, trajectory studies were conducted. Quasiclassical direct-dynamics trajectories were initiated from the area of **13<sup>‡</sup>**, a conformational analog of **13<sup>‡</sup>**, and a configurational analog derived from **8-ax**. The choice of TSs used was based on the two lowest-energy **11<sup>‡</sup>** analogs for addition to **8-eq** and the lowest-energy analog for addition to **8-ax**. Each normal mode was given its zero-point energy, a Boltzmann-random distribution of thermal energy appropriate for 298.15 K, and a random phase. The trajectories were integrated in 1-fs steps forwards and backwards in time using a Verlet algorithm, and were continued until they terminated at **9** / **10** or returned to intermediate **12**.

A striking feature of the trajectories is that the ring-contraction and boron-alkyl shifts are separated in time, eschewing any degree of synchronicity.<sup>17</sup> An average time of 216 fs was required to traverse from **13<sup>‡</sup>** to **9-I** / **9-R**. This includes on average 78 fs to get to **14** (defined as C<sub>2</sub>–C<sub>6</sub> < 1.6 Å with C<sub>1</sub>–C<sub>ethyl</sub> > 2.3 Å), 107 fs in the area of **14**, and 31 fs for the final highly exothermic boron-alkyl shift (defined by the C<sub>1</sub>–C<sub>ethyl</sub> distance reaching an approximate no-return

threshold of  $< 2.3$  Å). Only 5% of the trajectories involve temporal overlap between the ring contraction and boron-alkyl shifts, as judged by a  $C_1$ - $C_{\text{ethyl}}$  distance of less than 2.3 Å before the  $C_2$ - $C_6$  distance reaches  $< 1.6$  Å. The remaining 95% of trajectories involve well-separated stages for the ring contraction and boron-alkyl shift, remaining on the edge of an energy cliff near **14** for a remarkable 113 fs on average.

Table 1 summarizes the stereochemical results. For both **8-eq** and **8-ax**, the inversion products (**9-I** and **10-I**) were strongly favored, but in each case significant amounts of the retention products were formed. Due to the practicality-limited number of trajectories, the 95% confidence limits on the trajectory ratios are 2.0% and 3.0% for **8-eq** and **8-ax**, respectively. The trajectories overestimate slightly the amount of inversion, but the predicted ratios are within error of the experimental observations.

**Table 1.** Trajectory results starting from **13<sup>‡</sup>**, a low-energy conformational analog, and an **8-ax**-derived analog.<sup>a</sup>

System	Inversion ( <b>9-I</b> / <b>10-I</b> )	Retention ( <b>9-R</b> / <b>10-R</b> )	Ratio
<b>8-eq</b> , TS <b>13<sup>‡</sup></b>	360	30	92.3 : 7.7
2 <sup>nd</sup> -lowest TS	328	32	91.1 : 8.9
		weighted: 91.7 : 8.3 ( $\pm 2.0$ )	
		experiment: 90 : 10	
<b>8-ax</b> , lowest-energy TS	373	42	89.9 : 10.1
		( $\pm 3.0$ )	
		experiment: 87 : 13	

<sup>a</sup>See the SI for the TS structures and error analysis.

The trajectory results and their close fit with experimental observations support our hypothesis that the reaction involves a bifurcating energy surface and that the inversion and retention products arise from the same ring-contraction transition state. After the ring contraction, a sharply downward-sloping energy surface can lead from **14** to either product. The interesting question then is not why some retention is observed, but rather why inversion is so strongly favored.

We considered first whether the inversion-engendering ethyl group ( $\text{Et}_i$ , Figure 3) was initially better aligned with the empty p-orbital of  $C_1$  than the alternative ethyl group leading to retention ( $\text{Et}_r$ ). The migration of  $\text{Et}_i$  would then be favored by a steeper, least-motion path. Trajectories, however, initially place the  $\text{Et}_i$  and  $\text{Et}_r$  in nearly equivalent positions with respect to  $C_1$  in the area of **14**. A continuation of  $C_1$  and  $C_2$  motions in the transition vector for **13<sup>‡</sup>** (Figure 3) brings the  $C_1$ - $C_2$  bond and the non-migrating ethyl group ( $\text{Et}_n$ ) into a surprisingly encumbered eclipsed conformation (average  $C_2$ - $C_1$ -B- $\text{Et}_n$  dihedral angle  $-4^\circ$  with  $\sigma=11^\circ$ ) as the trajectories reach **14**. The slightly advantageous alignment of  $\text{Et}_i$  is ephemeral as conformational twisting continues, so that the 93% of the trajectories at some point in the area of **14** have  $\text{Et}_r$  better aligned. Dihedral alignment then cannot account for predominant inversion.

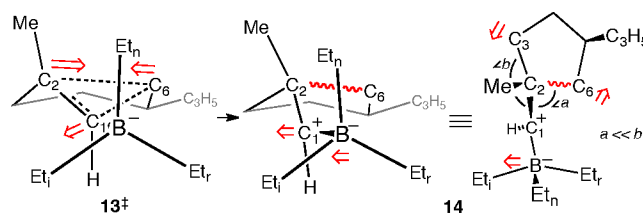


**Figure 3.** Composite conformational motion as **13<sup>‡</sup>** descends to **14** and **14** evolves with time.

The crux of the problem of understanding inversion is that the nominal structure of **14** (or **5**) is misleading. The symmetry of the bond connections to  $C_2$  makes the  $C_2$ - $C_6$  and  $C_2$ - $C_3$  bonds appear equivalent. (See the SI for evidence that the distant isopropenyl group has a negligible effect on the stereoselectivity.) However, **14** is actually highly asymmetric in three subtle but mutually reinforcing ways: (1) the newly formed  $C_2$ - $C_6$  bond is initially vibrationally excited, similarly to what has been seen in the acetone cation radical,<sup>3</sup> and it maintains this local excitation with a time constant of  $\sim 50$  fs, with some energy retained for up to 160 fs (see the SI); (2) the empty p-orbital of  $C_1$  is initially lined up with the  $C_2$ - $C_6$  bond, and donation from the electrons of the excited bond to  $C_1$  is retained for an extended time; (3) the  $\text{Et}_3\text{B}$  group as a whole is initially much closer to  $C_6$  than  $C_3$  ( $C_6$ -B averages  $\sim 3.1$  Å,  $C_3$ -B averages  $\sim 4.1$  Å) and the inertial effect of the  $\text{Et}_3\text{B}$  holds  $C_1$  closer to the  $C_2$ - $C_6$  bond.

These effects and their dissipation can be seen in the slow evolution of the average  $C_1$ - $C_2$ - $C_6$  and  $C_1$ - $C_2$ - $C_3$  angles after the formation of **14** (Figure 4). For trajectories that lead to the inversion product, the average  $C_1$ - $C_2$ - $C_6$  angle increases and the  $C_1$ - $C_2$ - $C_3$  angle decreases over time, but the system never reaches approximate symmetry, even after 200 fs. In contrast, the retention product is associated with trajectories that symmetrize the connections to  $C_2$  more rapidly. A low  $C_1$ - $C_2$ - $C_6$  angle prevents formation of the retention product. This is understandable as a short-lived steric effect in which the  $C_6$  methylene blocks a migrating  $\text{Et}_r$ . Inversion is then favored because  $\sim 80\%$  of the trajectories retain asymmetric geometries throughout their time in the area of **14**.

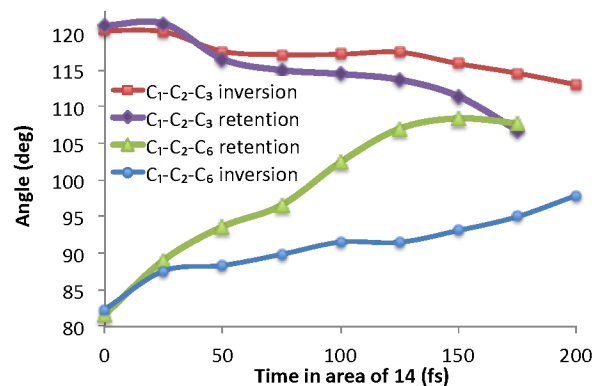


**Figure 4.** Evolution of the average  $C_1$ - $C_2$ - $C_6$  and  $C_1$ - $C_2$ - $C_3$  angles in inversion and retention trajectories after formation of **14**.

Symmetry and time are intimately intertwined. Chiral atropisomers are defined by the long time required for their racemization, while the rapidly inverting ethylmethylamine is

“operationally” achiral.<sup>1</sup> Most ‘memory effects’ impact stereoselectivity through the time persistence of conformations.<sup>18</sup> On shorter, sub-picosecond time scale, dynamic matching arises when the symmetry of a short-lived formally symmetrical intermediate is broken by the retained non-symmetrical momentum of the atoms as they enter the area of the intermediate. The general idea here is the same, but it is taken to its logical extreme since **14** is not an intermediate and since the molecular asymmetry is both energetic and geometrical.<sup>19</sup>

When the products of a reaction are selected within a sufficiently short time, symmetry all but disappears. As a result, molecular events that are separated in time can be interconnected by short-lived dynamical differences. This possibility is not new,<sup>2,3</sup> but here it affects the stereochemistry of an ordinary reaction in solution. This *dynamical asymmetry* complicates the understanding of stereochemical observations and their origin, since stereospecificity in formally concerted concomitant bonding changes would not necessarily require any degree of temporal overlap. We are continuing to explore the impact of dynamical effects on the understanding of selectivity in reactions.

## ASSOCIATED CONTENT Supporting Information

The Supporting Information is available free of charge on the ACS Publications website.

Complete descriptions of experimental and computational procedures and structures (PDF).

## AUTHOR INFORMATION Corresponding Author

singleton@chem.tamu.edu  
oleg.larionov@utsa.edu

## Notes

The authors declare no competing financial interest.

## ACKNOWLEDGMENT

DAS thanks the NIH (Grant GM-45617) for financial support. Financial support to OVL by the Welch Foundation (AX-1788) and the NSF (CHE-1455061 and CHE-1625963) is gratefully acknowledged.

## REFERENCES

- (1) Mislow, K.; Bickart, P. An Epistemological Note on Chirality. *Isr. J. Chem.* **1976**, *77*, 15, 1-6.
- (2) Rynbrandt, J. D.; Rabinovitch, B. S. Intramolecular Energy Relaxation. Nonrandom Decomposition of Hexafluorobicyclopropyl. *J. Phys. Chem.* **1971**, *75*, 2164-2171.
- (3) Nummela, J. A.; Carpenter, B. K. Nonstatistical Dynamics in Deep Potential Wells: A Quasiclassical Trajectory Study of Methyl Loss from the Acetone Radical Cation. *J. Am. Chem. Soc.* **2002**, *124*, 8512-8513.
- (4) Carpenter, B. K. Dynamic Behavior of Organic Reactive Intermediates. *Angew. Chemie Int. Ed.* **1998**, *37*, 3340-3350.
- (5) Doubleday, C.; Suhrada, C. P.; Houk, K. N. Dynamics of the Degenerate Rearrangement of Bicyclo[3.1.0]hex-2-ene. *J. Am. Chem. Soc.* **2006**, *128*, 90-94.
- (6) Collins, P.; Kramer, Z. C.; Carpenter, B. K.; Ezra, G. S.; Wiggins, S. Nonstatistical dynamics on the caldera. *J. Chem. Phys.* **2014**, *141*, 034111.
- (7) Leber, P.; Kidder, K.; Viray, D.; Dietrich-Peterson, E.; Fang, Y.; Davis, A. Stereoselectivity in a series of 7-alkylbicyclo[3.2.0]hept-2-enes:

Experimental and computational perspectives. *J. Phys. Org. Chem.* **2018**, *31*, e3888.

(8) Debbert, S. L.; Carpenter, B. K.; Hrovat, D. A.; Borden, W. T. The Iconoclastic Dynamics of the 1,2,6-Heptatriene Rearrangement. *J. Am. Chem. Soc.* **2002**, *124*, 7896-7897.

(9) Doubleday, C. Jr.; Bolton, K.; Hase, W. L. Direct Dynamics Study of the Stereomutation of Cyclopropane. *J. Am. Chem. Soc.* **1997**, *119*, 5251-5252.

(10) (a) Jin, S.; Nguyen, V. T.; Dang, H. T.; Nguyen, D. P.; Arman, H. D.; Larionov, O. V. Photoinduced Carboborative Ring Contraction Enables Regio- and Stereoselective Synthesis of Multiply Substituted Five-Membered Carbocycles and Heterocycles. *J. Am. Chem. Soc.* **2017**, *139*, 11365-11368. (b) Nguyen, V. D.; Nguyen, V. T.; Jin, S.; Dang, H. T.; Larionov, O. V. Organoboron Chemistry Comes to Light: Recent Advances in Photoinduced Synthetic Approaches to Organoboron Compounds. *Tetrahedron* **2019**, *75*, 584-602.

(11) (a) Metiu, H.; Ross, J.; Silbey, R.; George, T. F. On symmetry properties of reaction coordinates. *J. Chem. Phys.* **1974**, *61*, 3200-3209. (b) Valtazanos, P.; Elbert, S. T.; Ruedenberg, K. Ring Opening of Cyclopropylidenes to Allenes: Reactions with Bifurcating Transition Regions, Free Internal Motions, Steric Hindrances, and Long-Range Dipolar Interactions. *J. Am. Chem. Soc.* **1986**, *108*, 3147-3149. (c) Kraus, W. A.; DePristo, A. E. Reaction dynamics on bifurcating potential energy surfaces. *Theor. Chem. Acta* **1986**, *69*, 309-322.

(12) Hare, S. R.; Tantillo, D. J. Post-Transition State Bifurcations Gain Momentum – Current State of the Field. *Pure Appl. Chem.* **2017**, *89*, 679-698.

(13) (a) Singleton, D. A.; Hang, C.; Szymanski, M. J.; Meyer, M. P.; Leach, A. G.; Kuwata, K. T.; Chen, J. S.; Greer, A.; Foote, C. S.; Houk, K. N. Mechanism of Ene Reactions of Singlet Oxygen. A Two-Step No-Intermediate Mechanism. *J. Am. Chem. Soc.* **2003**, *125*, 1319-1328. (b) Patel, A.; Chen, Z.; Yang, Z.; Gutierrez, O.; Liu, H. -w.; Houk, K. N.; Singleton, D. A. Dynamically Complex [6+4] and [4+2] Cycloadditions in the Biosynthesis of Spinosyn A. *J. Am. Chem. Soc.* **2016**, *138*, 3631-3634.

(14) (a) Thomas, J. R.; Waas, J. R.; Harmata, M.; Singleton, D. A. Control Elements in Dynamically-Determined Selectivity on a Bifurcating Surface. *J. Am. Chem. Soc.* **2008**, *130*, 14544-14555. (b) Bogle, X. S.; Singleton, D. A. Dynamic Origin of the Stereoselectivity of a Nucleophilic Substitution Reaction. *Org. Lett.* **2012**, *14*, 2528-2531. (c) Kelly, K. K.; Hirschi, J. S.; Singleton, D. A. Newtonian Kinetic Isotope Effects. Observation, Prediction, and Origin of Heavy-Atom Dynamic Isotope Effects. *J. Am. Chem. Soc.* **2009**, *131*, 8382-8383. (d) Wang, Z.; Hirschi, J. S.; Singleton, D. A. Recrossing and Dynamic Matching Effects on Selectivity in a Diels-Alder Reaction. *Angew. Chem. Int. Ed. Engl.* **2009**, *48*, 9156-9159. (e) Singleton, D. A.; Hang, C.; Szymanski, M. J.; Greenwald, E. E. A New Form of Kinetic Isotope Effect. Dynamic Effects on Isotopic Selectivity and Regioselectivity. *J. Am. Chem. Soc.* **2003**, *125*, 1176-1177.

(15) As is common for secondary cations. Hong, Y. J.; Tantillo, D. J. A Maze of Dyotropic Rearrangements and Triple Shifts: Carbocation Rearrangements Connecting Stemarene, Stemodene, Betaerdene, Aphidicolene, and Scopadulanol. *J. Org. Chem.* **2018**, *83*, 3780-3793.

(16) Seeman, J. I. Effect of Conformational Change on Reactivity in Organic Chemistry. Evaluations, Applications, and Extensions of Curtin-Hammett/Winstein-Holness Kinetics. *Chem. Rev.* **1983**, *83*, 83-134.

(17) Dewar, M. J. S. Multibond Reactions Cannot Normally be Synchronous. *J. Am. Chem. Soc.* **1984**, *106*, 209-219.

(18) (a) Zhao, H.; Hsu, D. C.; Carlier, P. R. Memory of Chirality: An Emerging Strategy for Asymmetric Synthesis. *Synthesis* **2005**, 1-16. (b) Griesbeck, A. G.; Mauder, H.; Stadtmüller, S. Intersystem Crossing in Triplet 1,4-Biradicals: Conformational Memory Effects on the Stereoselectivity of Photocycloaddition Reactions. *Acc. Chem. Res.* **1994**, *27*, 70-75. (c) Berson, J. A. Memory Effects and Stereochemistry in Multiple Carbonium Ion Rearrangements. *Angew. Chem. Int. Ed.* **1968**, *10*, 779-791. (d) For a shorter-lived memory effect retained in the dynamics, see: Ghigo, G.; Maranzana, A.; Tonachini, G. Memory Effects in Carbocation Rearrangements: Structural and Dynamic Study of the Norborn-2-en-7-ylmethyl-X Solvolysis Case. *J. Org. Chem.* **2013**, *78*, 9041-9050.

(19) For geometrical effects of short-lived solvent interactions, see (a)

Hare, S. R.; Pemberton, R. P.; Tantillo, D. J. Navigating Past a Fork in the Road: Carbocation- $\pi$  Interactions Can Manipulate Dynamic Behavior of Reactions Facing Post-Transition-State Bifurcations. *J. Am. Chem. Soc.* **2017**, *139*, 7485–7493. (b) Carpenter, B. K.; Harvey, J. N.; Glowacki,

D. R. Prediction of Enhanced Solvent-Induced Enantioselectivity for a Ring Opening with a Bifurcating Reaction Path. *Phys. Chem. Chem. Phys.* **2015**, *17*, 8372–8381.

